

An Analytic Model Predicting the Optimal Range for Maximizing 1-Hop Broadcast Coverage in Dense Wireless Networks

Xiaoyan Li, Thu D. Nguyen, and Richard P. Martin

{xili, tdnguyen, rmartin}@cs.rutgers.edu
Department of Computer Science, Rutgers University
110 Frelinghuysen Rd, Piscataway, NJ 08854, USA

Abstract. We present an analytic model to predict the optimal range for maximizing 1-hop broadcast coverage in dense ad-hoc wireless networks, using information like network density and node sending rate. We first derive a geometric-based, probabilistic model that describes the expected coverage as a function of range, sending rate and density. Because we can only solve the resulting equations numerically, we next develop extrapolations that find the optimum range for any rate and density given a single precomputed optimum. Finally using simulation, we show that in spite of many simplifications in the model, our extrapolation is able to predict the optimal range to within 16%.

1 Introduction

We consider the problem of how networks of extremely dense embedded devices connected by a wireless network can set their output power to maximize the number of 1-hop receivers of a broadcast message. Many recent protocols proposed for use in ad-hoc wireless networks, such as directed diffusion [2] and ad-hoc positioning [8], rely on periodic broadcasts. In addition, many protocols, such as code propagation [6] and dynamic source routing (DSR) [3] rely on aperiodic broadcasts. Indeed, the fundamental broadcast nature of wireless networks makes broadcast an ideal building block for the discovery, routing and localization functions, which will be critical for future ad-hoc wireless systems.

At the same time, as technology trends continue to reduce the size, power consumption and cost of embedded wireless network devices, the scale of the networks built with them will continue to grow. For example, sensors are rapidly approaching the small size and low cost necessary for novel usage such as *active tagging*, i.e., representing the state of common everyday objects such as furniture, pens, and books. Our initial measurements of a common indoor environment for the active tagging application show that the average degree of such a network could easily range up to several hundred.

Given the high densities of these future sensor networks, a resulting challenge for applications using broadcast will be how to manage channel capacity to ensure good performance in terms of throughput, fairness and broadcast coverage. This challenge arises because if all nodes act greedily, using the maximum range, the channel will collapse; that is, the likelihood of any neighbors receiving the message correctly quickly

approaches zero in dense networks due to collisions. As shown in [6], many protocols perform poorly as density increases because of this issue.

We are thus motivated to consider how devices in these networks can maximize the number of 1-hop receivers of a broadcast message. We refer to *broadcast* as the 1-hop message, as opposed to *flooding* which intends to cover all the nodes via multi-hop forwarding. We choose to examine broadcast coverage because it is an important metric for protocols using broadcast as a building block. In addition, a network without good broadcast coverage is unlikely to have good throughput or latency properties — if many nodes fail to receive a broadcast message they would most likely have trouble receiving a normal unicast message due to the fundamental channel properties (i.e., a single sender impacts many receivers) of wireless transmission.

Our approach centers on the *spatial reuse* of wireless resources. Specifically, given the surrounding sending rate, node density, and a simple geometric model of wireless communication to compute the radio range, each node can just set its range to the optimal value, which probabilistically maximizes the 1-hop *coverage* for a broadcast packet. We use radio range as a parameter because it is more tractable to analyze than output power directly; adjusting output power to achieve the computed optimal range is future work.

To derive our analytic approach, we first build a geometric model that predicts the likelihood of a collision given all nodes in a uniform density network broadcasting at the same rate using the same range. Using this model we can numerically solve for the optimal range for any combination of density and broadcast rate. Unfortunately, we cannot use the above model analytically since the optimal range is not easily computable using a closed-form formula. Thus, we next introduce two relations from which we can build an extrapolation that can be used in real-time to compute a range setting that is close to optimal based on information about the local density and sending rate. We show that simplifying assumptions made in deriving the model and the inexactness of one of the extrapolation relations leads to at most 16% error in estimating the optimal range.

We argue that our analytic approach is quite applicable to small wireless devices because of its simplicity; the complexity is buried offline in the numeric solver leaving the nodes to only perform the lighter weight extrapolation. In addition, we believe that estimations of the local density and sending rate are possible via local observations on the transmission channel. For example, distances to neighbor nodes can be computed using signal strength [1] or signal timing-differential approaches [9]. We leave the exact nature of density estimation as future work.

The rest of this paper are organized as following: In Section 2, we construct the geometric model. Section 3 introduces the extrapolation method. In Section 4 we evaluate the approach via simulation. We compare and contrast our work to related work in Section 5. Finally, in Section 6 we conclude.

2 Model Construction

In this section, we develop an analytic model to derive optimal transmission range based on the sending rate and node density. For simplicity, we develop only a two-dimensional

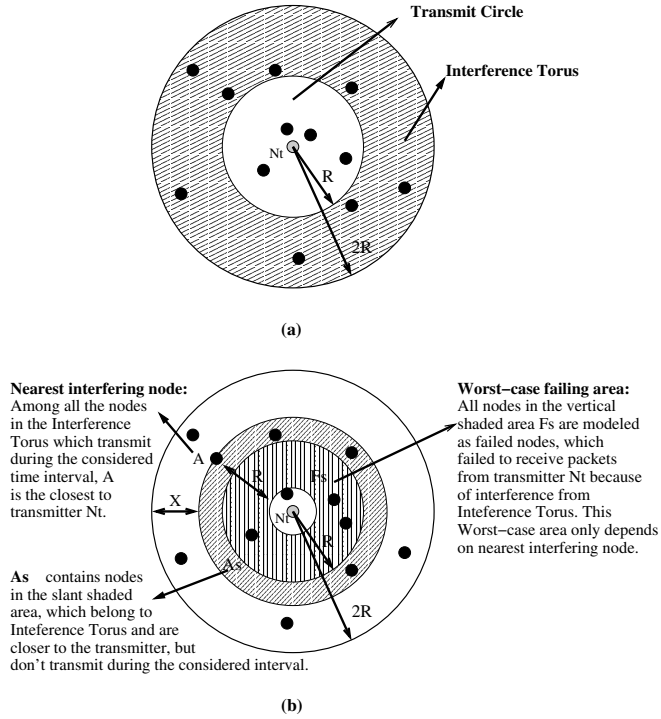


Fig. 1. Definitions and assumptions behind the derivation of our model in 2 dimensions. (a) shows the basic setup of our model, where N_t is the transmitting node, the white circle encapsulate nodes that should receive a transmission from N_t , called the transmit circle, and the slant-shaded area contains nodes that can interfere with the reception of N_t 's packet. (b) shows what happens when a node A interferes with N_t 's transmission causing some nodes in the transmit circle to fail. Here we assume that A is the interfering node closest to N_t , with distance X from the outer circle ($2R$) of the interference torus.

model; extending the model to three-dimensions is straightforward. (All our simulations run in the full three dimensions.)

We use a set of assumptions to make an analytic solution tractable: (1) nodes are spatially distributed according to a Poisson distribution with an average density of λ_s ; (2) applications running on each node generate packets to send according to a Poisson distribution with average rate λ_p ; (3) all packets are of the same length and take time T to transmit; and, (4) all nodes use a CSMA protocol. We also use a fairly simple wireless communication model similar to the one in [11]: all nodes have the same radio range, where nodes within R distance from a transmitter will detect the packet transmission while those further away will not. More than one packet transmission within distance R to a receiver will cause collision and all overlapped packets at the receiver are corrupted.

Figure 1 shows the geometric reasoning underlying our model, which derives the expected coverage for a particular transmitter given the assumptions listed above. We call the area within distance R of the transmitter the *transmit circle*. During a packet transmission, nodes inside the transmit circle will detect the transmission and thus be blocked from transmitting via CSMA. Transmissions from within the *interference torus* (the slant shaded area bounded by circles with radius R and $2R$ from the transmitter, shown in Figure 1 (a)) will have a similar effect as hidden terminals, interfering with the receipt of the packet for some of the nodes in the transmit circle. We assume that the sending rates of nodes in the interference torus are not affected by CSMA; that is, transmission for each of those nodes is still independently defined by a Poisson distribution. This assumption means that we do not have to consider nodes that are further than $2R$ away from the transmitter, since their only effect on the nodes under consideration is through CSMA. This assumption is conservative since CSMA effectively slows down the sending rate, implying that the model will overestimate the number of interfering packets.

We call a node within the transmit circle that does not correctly receive the transmitted packet a *failed* node. Thus, we model packet coverage as the number of nodes that can detect a particular packet transmission minus failed nodes, which gives the following equation:

$$E(C) = \lambda_s(\pi R^2) - E(\text{number of failed nodes})$$

where $\lambda_s(\pi R^2)$ is just the expected number of nodes in the transmit circle. As can be seen, the task of modeling coverage really becomes a task of deriving the number of failed nodes. An exact derivation, however, would be quite challenging because in the general case, we would have to account for multiple overlapping circular interference regions caused by colliding transmissions from the interference torus. One method to make the analysis tractable is to assume that if a node with distance d to the transmitter fails, then all nodes i with distance $d_i \geq d$ also fail. This assumption effectively means that the modeled total failing area (shown as the vertically shaded *worst-case failing area* in Figure 1 (b)) will be decided by the distance from the transmitter to the *nearest interfering node*. Clearly this simplification is conservative; the modeled failing area will always be larger than or equal to the true failing area. However, the worst-case failing area computation is now easily tractable.

Let X be a random variable that represents the distance from the nearest interfering node (A in Figure 1(b)) to the outer ring of the torus. Let A_s (the slant shaded area in Figure 1(b)) be the area of the Interference torus containing nodes which are closer to the transmitter than A is to the transmitter, such that

$$A_s = \pi((2R - x)^2 - R^2)$$

Then, the CDF for X is:

$$P(X \leq x) = \sum_{k=0}^{\infty} \left[P(k \text{ nodes in } A_s) (P(\text{a node does not transmit for } 2T))^k \right]$$

It gives the probability that the closest interfering node is at least $(2R - x)$ away from the transmitter; i.e., the probability that no nodes within A_s transmit during the current

transmission. (We use $2T$ as the bounding time range since unslotted CSMA needs both the current transmission period T and the previous T period to be quiet for a successful reception.) Substituting in the appropriate parameters, this equation becomes

$$\begin{aligned}
P(X \leq x) &= \sum_{k=0}^{\infty} \left[\left(\frac{(\lambda_s A_s)^k e^{-\lambda_s A_s}}{k!} \right) (e^{-\lambda_p 2T})^k \right] \\
&= e^{-\lambda_s A_s} \sum_{k=0}^{\infty} \left[\frac{(\lambda_s A_s e^{-\lambda_p 2T})^k}{k!} \right] \\
&= e^{-\lambda_s A_s} e^{\lambda_s A_s e^{-\lambda_p 2T}} \\
&= e^{-\lambda_s A_s (1 - e^{-\lambda_p 2T})} \tag{1}
\end{aligned}$$

Thus, the expected number of failed nodes in the worst case can be readily computed as:

$$NF_w = \int_0^R [\lambda_s \pi (R^2 - (R - x)^2) P(x \leq X \leq x + dx)] \tag{2}$$

where $\pi(R^2 - (R - x)^2)$ represents the *worst-case failing area* (shown as the vertical shaded area in Figure 1(b)).

As mentioned above, approximating the failing area with *worst-case failing area* is conservative. Particularly, when there are very few interfering transmitters, this simplification is too conservative, and thus unable to provide a good approximation. To account for the inaccuracy, we set a threshold for the expected number of interfering transmitters. Only when the expected number reaches this threshold, we use the worst-case failing area as the modeled failing area; otherwise we use portions of the worst-case failing area.

To compute the expected number of interfering transmitters, we need to derive an expression for the *aggregate sending rate* given an average node density λ_s and average individual sending rate λ_p . Recall that we model the transmission at each node as an independent Poisson process with intensity λ_p , which will transmit with probability $1 - e^{-\lambda_p t}$. Given a density, the aggregate sending rate observed per unit area then is simply $\lambda_s(1 - e^{-\lambda_p t})$. Thus the expected number of interfering transmitters is the aggregate transmission from the interference torus area:

$$E(Tr) = \lambda_s(1 - e^{-\lambda_p 2T})\pi((2R)^2 - R^2) \tag{3}$$

We derive the interfering transmitters threshold by assuming all the interfering transmitters sit in the middle of the interference torus radius ¹ (i.e., $\frac{3}{2}R$ to the center of the transmit circle). We can then compute the worst-case failing area and the interfered area from a single interfering transmitter respectively. The ceiling for the quotient

¹ Through similar simulation validations as in Section 4 we find that assuming the interfering transmitters are in the middle of the interference torus area/volume would give a better approximation, but that underestimates the collisions in a few cases, which is not conservative with respect to R.

of these two areas is used as the threshold. The threshold for 2 dimensions is 6^2 , and for 3 dimensions is 11.

Finally, we complete the model as the following piecewise function:

$$E(C) = \begin{cases} \lambda_s(\pi R^2) - \frac{E(Tr)}{6}NF_w & E(Tr) < 6 \\ \lambda_s(\pi R^2) - NF_w & E(Tr) \geq 6 \end{cases} \quad (4)$$

3 Practical Usage of the Model

The model we have just derived gives us a mathematical means to estimate the coverage given λ_s , λ_p and T . Unfortunately, the final result is not a closed form formula and so requires numeric methods to find the R value (R_o) that maximizes the coverage. This makes it impractical for the embedded devices to use the model directly at run-time. Thus, in this section, we derive two relations that will allow us to find any R_o given a single pre-computed R_o for a particular tuple of $(\lambda_s, \lambda_p, T)$. These extrapolations thus make it tractable to find R_o in the context of a running protocol stack on resource-constrained devices.

3.1 Relating Density to Coverage

We begin by deriving a relationship between the expected coverage of two scenarios with the same sending rate (λ_p) but different densities (λ_s). In particular, given two scenarios $(\lambda_{p1}, \lambda_{s1}, R_1)$ and $(\lambda_{p2}, \lambda_{s2}, R_2)$ with the same sending rate, the expected coverage between the two scenarios is the same when the ranges encircle the same expected number of nodes. Specifically:

$$\lambda_{p1} = \lambda_{p2}, \lambda_{s1}R_1^2 = \lambda_{s2}R_2^2 \Rightarrow E(C_1) = E(C_2) \quad (5)$$

To show that the above relationship holds, observe that since $\lambda_{s1}R_1^2 = \lambda_{s2}R_2^2$, the two scenarios are geometrically identical given our model represented by Figure 1. That is, the expected number of nodes in the transmit circle and in the interference torus are exactly the same across the two scenarios. Further, since all nodes are spatially distributed according to a Poisson distribution and have the same packet sending rate, λ_p , we can conclude that each node's transmission will be equally affected in the two cases, which means that the expected coverage in the two cases will be the same.

3.2 Relating the Sending Rate to Coverage

Having derived a relationship between density and coverage, we now consider the other dimension, the sending rate. The intuition is to derive a relationship describing the expected coverage change as we vary the number of interfering transmissions while keeping the range constant.

² For 2 dimensions, the worst-case failing area in this case is $\frac{3}{4}\pi R^2$. For 2 circles with radius R and the centers d apart ($d < 2R$), the intersection area can be computed as $(2R^2 \cos^{-1}(\frac{d}{2R}) - \frac{d}{2}\sqrt{4R^2 - d^2})$. Thus, the interfered area from a single interfering transmitter is $(R^2(\cos^{-1}(\frac{3}{4}) - \frac{3\sqrt{7}}{8}))$. So the threshold is $\lceil 5.19 \rceil = 6$.

We have shown in Section 2 that given an average node density λ_s and average individual sending rate λ_p , the aggregate sending rate observed per unit area is simply $\lambda_s(1 - e^{-\lambda_p t})$. Now, given two scenarios $(\lambda_{p1}, \lambda_{s1}, R_1)$ and $(\lambda_{p2}, \lambda_{s2}, R_2)$, we wish to show that

$$\lambda_{s1} (1 - e^{-\lambda_{p1} 2T}) = \lambda_{s2} (1 - e^{-\lambda_{p2} 2T}), R_1 = R_2 \Rightarrow \frac{E(C_1)}{E(C_2)} = \frac{\lambda_{s1}}{\lambda_{s2}} \quad (6)$$

To show that this relationship holds, observe that $E(C)$ as defined in equation 4 can be rewritten as:

$$E(C) = \lambda_s \pi \Psi(R, \lambda_s, \lambda_p), \text{ with } \Psi(R, \lambda_s, \lambda_p) = \begin{cases} R^2 - \frac{E(Tr)}{6} \frac{NF_w}{\lambda_s \pi} & E(Tr) < 6 \\ R^2 - \frac{NF_w}{\lambda_s \pi} & E(Tr) \geq 6 \end{cases}$$

Since $\lambda_{s1}(1 - e^{-\lambda_{p1} 2T}) = \lambda_{s2}(1 - e^{-\lambda_{p2} 2T})$ and $R_1 = R_2$, combining the above equation with equations 1, 2 and 3 shows that the $\Psi(R, \lambda_s, \lambda_p)$ portion of the above equation is the same for the two scenarios. Thus, we conclude that $\frac{E(C_1)}{E(C_2)} = \frac{\lambda_{s1}}{\lambda_{s2}}$.

Note that since the effect of CSMA on the observed aggregate sending rate changes with the density, our assumption of independent transmission rate in the interference torus translates to different levels of inaccuracy for different densities. Thus, the relationship just derived is not exact, whereas the first relationship is exact.

3.3 Extrapolation Using the Derived Relations

We now show how the above two relations can be used to find the optimal transmission range R_o for an arbitrary network defined by the tuple $(\lambda_s, \lambda_p, T)$.

As described in Section 1 and verified in our experiments, the curve plotting expected coverage against the transmission range in a specific setting would follow a bell shape. The range corresponding to the maximum expected coverage is the R_o for this specific setting.

Using equation 5, if we keep λ_p fixed while changing λ_s to λ'_s , then

$$E(C(\lambda'_s, \lambda_p, r')) = E(C(\lambda_s, \lambda_p, r)), \text{ where } \lambda'_s r'^2 = \lambda_s r^2$$

In essence, when we increase λ_s , the bell curve moves left and becomes sharper; when we decrease λ_s , the curve moves right and becomes flatter. However, the curve will remain bell shaped such that the new R'_o is given by

$$R'_o = \sqrt{\frac{\lambda_s R_o^2}{\lambda'_s}} \quad (7)$$

Using equation 6, if we change both λ_p and λ_s but keep $\lambda_s(1 - e^{-\lambda_p 2T})$ as well as R constant, then the expected coverage for each transmission range value will scale according to

$$E(C(\lambda'_s, \lambda'_p, r)) = E(C(\lambda_s, \lambda_p, r)) \frac{\lambda'_s}{\lambda_s}, \text{ where } \lambda_s (1 - e^{-\lambda_p 2T}) = \lambda'_s (1 - e^{-\lambda'_p 2T})$$

The above relation means that the new curve for expected coverage will change along the y-axis but not the x-axis: it will shrink when we decrease λ_s and grow when we increase λ_s . So, the original R_o will still correspond to the maximum coverage, i.e.:

$$\lambda_s(1 - e^{-\lambda_p 2T}) = \lambda'_s(1 - e^{-\lambda'_p 2T}) \Rightarrow R'_o = R_o \quad (8)$$

Putting the above reasoning together, if we know R_{o1} for a particular tuple $(\lambda_{s1}, \lambda_{p1})$, then we can compute R_{o2} for any other tuple $(\lambda_{s2}, \lambda_{p2})$, assuming that packets are of the same size and so T stays constant. This computation, which is just an extrapolation along the dual dimensions of λ_s and λ_p , is done as follows. Let

$$\lambda_{p3} = \lambda_{p1} \quad \text{and} \quad \lambda_{s3}(1 - e^{-\lambda_{p3} 2T}) = \lambda_{s2}(1 - e^{-\lambda_{p2} 2T})$$

Then, using equations 7 and 8, we can compute that

$$R_{o3} = \sqrt{\frac{\lambda_{s1} R_{o1}^2}{\lambda_{s3}}} \quad \text{and} \quad R_{o2} = R_{o3}$$

Thus,

$$R_{o2} = \sqrt{\frac{\lambda_{s1} R_{o1}^2}{\lambda_{s3}}} = \sqrt{\frac{\lambda_{s1} (1 - e^{-\lambda_{p1} 2T}) R_{o1}^2}{\lambda_{s2} (1 - e^{-\lambda_{p2} 2T})}}$$

shows that we can derive the optimal transmission range for any tuple (λ_s, λ_p) given a known optimal range for one such tuple. In the remainder of the paper, we will use C_o to denote the quantity $\lambda_{s1} (1 - e^{-\lambda_{p1} 2T}) R_{o1}^2$.

4 Model Validation

We now proceed to quantify the error introduced by the various simplifying assumptions that make the derivation and analysis of the model tractable; specifically: (1) the assumption that sending rates of nodes in the interference torus are not affected by CSMA, and (2) approximating the failing area with portions of the whole worst-case failing area. We use a simulation-based approach, where we simulate a large number of scenarios and then compare the observed optimal range with that predicted by the model. In particular, our simulator captures the rate-limiting effect of CSMA and there is no approximation involved in counting successful or failed receptions. We shall see that under a wide range of conditions, the modeling error never results in a range prediction error of more than 16%.

Our validation process is as follows: We first numerically solve C_o for a number of different (λ_s, λ_p) tuples with a constant T (0.04 sec.). Although our extrapolations are not exact, we found that all the numerically computed C_o values agreed to within 4 digits, and thus we always use $C_o = 0.188$. Next, we simulated various network scenarios to empirically find the optimal R_o for different settings of (λ_s, λ_p) and compare them against the ones computed using extrapolation from C_o . To find the empirical R_o , we experimentally plot the coverage vs. range curve while varying R to find the one that

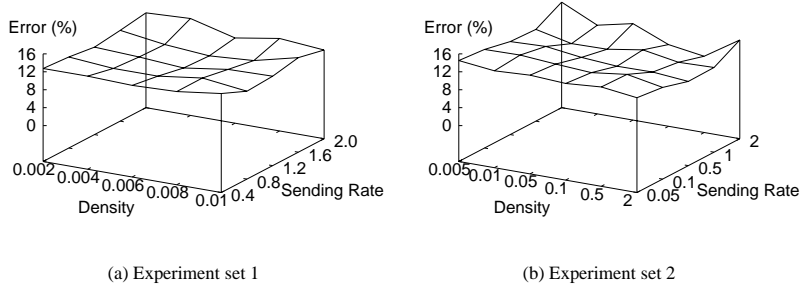


Fig. 2. Validation results. The Figure shows the percentage difference in the optimal ranges, obtained via simulation and analytic model, vs. density and sending rate.

maximizes coverage. (In both experiment sets, the explored granularity for transmission ranges is 0.1m.)

Our simulator models 3 dimensional spaces. The network configuration and wireless communication follow the same basic model as described in Section 2. To account for boundary effects, we implemented spatial wrap-around, where transmissions propagate at the edge of the space as if space is a torus. In all of the experiments, we make sure that the tested range is fairly small compared to the modeled space so that the spatial correlations resulted from wrap-around do not significantly affect the results.

Figure 2 presents our validation results, showing the percentage difference in the optimal range obtained via simulation and the analytic model; here the analytic model always under-predicts the range, which we believe to be good since a small under utilization of the channel is preferable to an over-aggressive range setting that could lead to channel collapse.

Experiment set 1 corresponds to a small fraction of the parameter space, which allows us to extensively test each point. All the experiments in set 1 ran in a $100 \times 100 \times 100m^3$ volume. Each parameter setting is tested with multiple spatial configurations. Specifically, 10 randomized configurations if the number of nodes is less than 5000; otherwise 5 configurations. The experiments ran until the time when each node is expected to have sent 50 messages. The final coverage for a particular setting is averaged over all nodes.

Experiment set 2 corresponds to broader settings along both λ_s and λ_p dimensions, covering most practical scenarios (Notice the axes in Figure 2(b) are not linear). Compared to experiment set 1, this set extends to much higher densities and slower sending rates. However, because some of the settings require simulating tens of thousands nodes we have not been able to test each point as extensively as we did for set 1. For example, the simulations are run on only one spatial configuration. We believe the average over the large number of nodes involved in each simulation will average out the effects of these limitations.

In all, our validation shows that the extrapolation can predict R_o to within 16%. We believe that this is reasonably accurate for applying our model to real practical settings.

5 Related Work

We categorize related work into three general areas: topology control, MAC layer improvements, and analytic modeling.

Topology Control While all the range adjustment to control topology work below improves spatial reuse, their more prominent goal has been energy conservation while maintaining connectivity. Our work does not consider energy use; we instead maximize the 1-hop broadcast coverage at the expense of energy. Our work also does not provide connectivity guarantees.

The work in [10] formulated topology control as an optimization problem and provided a centralized algorithm to find the minimum power that should be used by each node to achieve the objective. [12] used an orientation approach, where each node keeps increasing its range until the collected orientation information guarantees connectivity. The algorithm in [5] works closely with the routing layer rather than at the MAC layer. By locally comparing the multiple routing tables, a node could choose the minimum power level needed to forward a packet. A variety of centralized or distributed scheduling methods [13] have been used to control the topology for wireless networks. However, we consider centralized approach prohibitive in dense wireless sensor networks. In addition, the above distributed reservation approach relies on feedback, which is impossible to manage for broadcast messages that we considered here.

MAC layer improvements Typical 802.11 MAC layers use RTS and CTS control packets set at maximal power to eliminate the hidden terminal problem. RTS/CTS schemes lower spatial reuse by blocking possible concurrent transmissions. One scheme [4] proposed to transmit data packets at the minimum required power level thus reducing energy use, however, there was no spatial reuse improvement. Another work [7] proposed a separate busy tone channel, which was used by each node to advertise the additional noise level that could be accommodated and thus could support more concurrent transmissions, i.e., better spatial reuse. Instead of modifying the MAC layer directly, our range control scheme could work between the MAC and routing layers.

Analytic Modeling The analytic modeling work most related to ours is [11], which found the optimum degree where packet forwarding would have the best expected progress. Our analytic modeling methods are similar in that we reason about the best expected likelihood of packet reception.

6 Conclusion

In this work we presented an analytic model for ad-hoc wireless networks to predict the optimal range to maximize the 1 hop broadcast coverage. Our approach is in effect performing topology control on the broadcast packets. Unlike most topology control approaches, however, we took a geometric rather than a graph theoretic approach to reason about the impact of the effects of range on coverage.

We developed a geometric-based analytic model that describes the relationship between sending rate, density, range and coverage. Although our model is not a closed-form solution, we presented a simple method to extrapolate the optimal range given a node's local sending rate and density observations. Through simulations we demonstrated that despite its numerous simplifications, the model predicts the optimal range setting to within 16% across an order of magnitude set of rates and densities which could be realistically found in these networks.

References

1. J. Hightower, C. Vakili, G. Borriello, and R. Want. Design and Calibration of the SpotON Ad-Hoc Location Sensing System, unpublished., 2001.
2. C. Intanagonwiwat, R. Govindan, and D. Estrin. Directed Diffusion: A Scalable and Robust Communication Paradigm for Sensor Networks. In *Proceedings of the Sixth Annual International Conference on Mobile Computing and Networking*, Boston, MA, Aug. 2000.
3. D. Johnson and D. Maltz. Dynamic Source Routing in Ad Hoc Wireless Network. In *Proceedings of the 4th Annual ACM/IEEE International Conference on Mobile Computing and Networking (Mobicom)*, Rye, New York, Nov. 1996.
4. E.-S. Jung and N. Vaidya. A Power Control MAC Protocol for Ad Hoc Networks. In *ACM International Conference on Mobile Computing and Networking*, 2002.
5. V. Kawadia and P. R. Kumar. Power Control and Clustering in Ad Hoc Networks. In *INFOCOM*, 2003.
6. P. Levis, N. Patel, D. Culler, and S. Shenker. Trickle: A Self-Regulating Algorithm for Code Propagation and Maintenance in Wireless Sensor Networks. In *First Symposium on Network Systems Design and Implementation (NSDI)*, Mar. 2004.
7. J. Monks, V. Bharghavan, and W. mei W. Hwu. A Power Controlled Multiple Access Protocol for Wireless Packet Networks. In *INFOCOM*, pages 219–228, 2001.
8. D. Niculescu and B. Nath. Ad hoc positioning system (APS). In *GLOBECOM (1)*, pages 2926–2931, 2001.
9. N. Priyantha, A. Chakraborty, and H. Balakrishnan. The Cricket Location-Support system. In *ACM International Conference on Mobile Computing and Networking (MobiCom)*, Boston, MA, Aug. 2000.
10. R. Ramanathan and R. Hain. Topology Control of Multihop Wireless Networks Using Transmit Power Adjustment. In *INFOCOM (2)*, pages 404–413, 2000.
11. H. Takagi and L. Kleinrock. Optimal Transmission Ranges for Randomly Distributed Packet Radio Terminals. *IEEE Transactions on Communications*, 32(3):246–257, March 1984.
12. R. Wattenhofer, L. Li, P. Bahl, and Y.-M. Wang. Distributed Topology Control for Wireless Multihop Ad-hoc Networks. In *INFOCOM*, pages 1388–1397, 2001.
13. C. Zhu and M. S. Corson. A Five-phase Reservation Protocol (FPRP) for Mobile Ad Hoc Networks. In *Wireless Networks*, July 2001.